“BABEȘ-BOLYAI” UNIVERSITY CLUJ-NAPOCA

Faculty of Biology and Geology

Doctoral School of Integrative Biology

Doctoral thesis

Summary

PhD Coordinator:
Prof. Dr. Marcel PÂRVU

PhD Student:
Cristina Lorena VĂCAR

Cluj-Napoca

2024

“BABEȘ-BOLYAI” UNIVERSITY CLUJ-NAPOCA

Faculty of Biology and Geology

Doctoral School of Integrative Biology

Doctoral thesis

Summary

Micromycetes involved in biodeterioration and bioremediation

PhD Coordinator:

Prof. Dr. Marcel PÂRVU

PhD Student:

Cristina Lorena VĂCAR

Cluj-Napoca

2024

Table of contents

Key words

Biodeteriorative enzymes, pigment solubilisation, metal contaminants, mycoremediation, metal resistance strategies, mercury, mercury biovolatilization.

CHAPTER I

Data from literature

Micromycetes represent a highly diverse group of microscopic fungi bringing forward both challenges and opportunities for humanity. Micromycetes prove resilience in their abiotic and biotic interactions, adapting to challenging environmental conditions by exploiting very diverse ecological niches. Uncovering fungal responses in complex environmental conditions and harnessing their potential benefits can serve for development of countless applications.

Biodeterioration is the irreversible alteration of the quality of objects of importance for humanity by various organisms and microorganisms (*e.g.*, plants, algae, insects, bacteria, fungi). Biodeterioration of patrimony artworks is a less considered topic that potentially jeopardizes the integrity of art objects of inestimable value. Conservation within heritage and museum buildings can be a challenging task, due to unfavorable indoor conditions and limitations of the disinfection procedures (Fermo and Comite, 2022). Fungal representatives were found to dominate the microorganisms' composition in museal environment air and surfaces (Skóra *et al.*, 2015). Moreover, fungi are more problematic than bacteria and play the most important role in biodeterioration of objects in museums, collections, and libraries (Kavkler *et al.*, 2022; Sterflinger and Piñar, 2013). Important yet scarce progress has been made in understanding the metabolic processes associated with micromycetes' biodeterioration of canvas paintings. Addressing aspects related to biodeterioration, such as the species involved and mechanisms of deterioration, is essential for contributing to the development of conservation strategies and disinfection technologies in the domain of patrimony artworks.

Bioremediation is a process that uses microorganisms, plants, or enzymes to degrade, detoxify, or remove contaminants from different substrates. Metal contaminants are the main contributors, to both soil and groundwater contamination in Europe (Panagos *et al.*, 2013). Toxic elements, such as As, Cd, Hg, Pb, or trace elements in toxic concentrations, Cu, Fe, Mn, Zn, can persist indefinitely in the environment. Mercury is an element of special concern for human health as it is highly mobile in the environment and tends to bioaccumulate and further biomagnify through food webs. Cellular toxicity to Hg occurs due to its high affinity for thiol groups of cysteine residues present in small molecules, like glutathione, or in enzymes, thus impairing their function. Areas around hot spots of Hg pollution require urgent interventions to reclaim environmental safety and reduce adverse effects on human health.

Conventional Hg remediation techniques, *e.g.*, encapsulation, vitrification, chemical immobilization, landfilling, soil washing, come at excessive cost, intense labour and with extreme soil disturbances (Rajendran *et al.*, 2022). These limitations encouraged the progress in the field of bioremediation, including phytoremediation, microorganisms-assisted phytoremediation, or mycoremediation, as tools for eco-friendly and sustainable remediation of landscapes affected by metals pollution. The integration of phytoremediation and microbial assistance emerged as an approach for development of innovative and sustainable remediation strategies for being cost-effective and ecological alternatives to conventional techniques (Wang *et al.*, 2020). Arbuscular mycorrhizal fungi and fungal endophytes can improve Hg phytoremediation by promoting plant growth and/or Hg uptake, especially in roots, although the molecular mechanisms involved in Hg mobilization from soil to plants remains to be elucidated. These dual functions are integral to the success of phytoremediation strategies aimed at mitigating metal contamination in soils (Tiodar *et al.*, 2021).

Mycoremediation is a type of bioremediation that employs fungi for removal, degradation, or toxicity reduction of numerous contaminants from diverse substrates. The progress of this biotechnology is incipient due to insufficient knowledge of the mechanisms of interaction between fungi and metals. Filamentous micromycetes are considered excellent candidates for metal contaminants remediation purposes, as they possess multiple relevant characteristics. High surface area of the cells with diverse negatively charged functional groups in the cell wall structure and production of organic acids with metal-binding properties are providing the first line of protection against toxic metals . In addition, the hyphae networks enable colonization of porous matrices of soils. At the cellular level, micromycetes harbour multiple antioxidant systems, plasma membrane and tonoplast metal transporters, metal-buffering molecules, and metal-speciating enzymes (Kumar and Dwivedi, 2021). Investigating the interaction of metals with micromycetes is important for advancing knowledge and applications in the field of microremediation of metal contaminants.

Two main types of mechanisms sustain micromycetes survival in the presence of toxic or excess metals: passive/ATP-independent, and active/ATP-dependent. Passive mechanisms prevent metal entry into the cells, by adsorption to the cell wall or sequestration by extracellular metabolites and are often associated with the term biosorption (Gadd, 2009). Active mechanisms, collectively named bioaccumulation, occur mostly intracellularly as metal transporters across

plasma membrane, cytosolic metal-induced binding molecules, or vacuolar compartmentation (Fomina and Gadd, 2014).

In addition to the passive biosorption and active bioaccumulation, biovolatilization was reported occasionally as a resistance strategy to Hg in fungi (Chang *et al.*, 2020; Chang *et al.*, 2019). The Hg^{2+} detoxification mechanism through biovolatilization was well-described in bacteria. The mercuric reductase (MerA) is a cytosolic homodimeric flavin disulfide oxidoreductase, which uses nicotinamide adenine dinucleotide (phosphate) (NAD(P)H) as reducing factor and flavin adenine dinucleotide (FAD) as cofactor (Lian *et al.*, 2014; Barkay *et al.*, 2003). MerA is the core enzyme responsible for the catalytic reduction of the highly reactive Hg^{2+} to volatile, relatively inert monoatomic Hg^0, which can readily escape the cell *via* diffusion through the cell membrane, thus avoiding cellular toxicity. However, the fungal Hg^{2+} reducing mechanism is not well understood, as thorough genetic and biochemical characterization of this enzyme were not documented.

Aim and objectives

The aim of the research undertaken within this doctoral thesis was to advance the understanding of micromycetes' role in the divergent processes of biodeterioration and bioremediation. The main objectives were to:

(1) assess the micromycetes' diversity and their deteriorative mechanisms involved in canvas paintings biodeterioration;

(2) characterize metal-resistant micromycetes for their metal bioremediation potential, with special emphasis on mercury (Hg), and establish primary metal-resistance strategies in a highly resistant micromycete.

CHAPTER II

Materials and methods

1. Biodeteriorative fungal community of canvas paintings

This study focused on analysing the diversity of culturable fungal community and metabolic processes involved in biodeterioration. The fungal isolates were recovered from five canvas paintings, dating from the 18^{th}-20^{th} centuries, comprising four oil on canvas artworks from The Art Museum, Cluj-Napoca, and one gouache on canvas painting from a private collection.

Sampling was carried out non-invasively under aseptic conditions, and the sampling supports were incubated on Czapek-Dox agar medium. Pure fungal colonies were obtained and used for molecular identification, and for screening of enzymatic activities and pigments solubilization capacity. Molecular identification was performed using the internal transcribed spacer (ITS), translation elongation factor-1 (TEF-1), or tubulin beta chain (Bt2) regions. The enzymatic activity screening was performed in specific culture media for lipases, esterases, lecithinases, caseinases, gelatinases, and amylases, and with API ZYM test strips, for a series of 19 enzymes. The pigment solubilisation/degradation capacity was assessed in culture medium individually amended with primary colours pigments, red, yellow, blue, white, and black, commonly used in paintings. To validate the acidification of the culture medium by organic acids secretion, as a possible mechanism for pigment degradation, bromothymol blue (pH 6 – yellow, pH 7.6 – blue) was added to the culture medium.

2. Metal-resistant fungal community from a Hg-contaminated site

This study aimed to isolate and characterize culturable micromycetes with bioremediation potential for metal contaminants. The fungal isolates were recovered from rhizosphere soil of plant species colonizing a contaminated site.

The study site, former chloralkali plant in Turda, Cluj County, Romania, with historical Hg contamination, was selected to perform soil sampling. The elemental content of the soil samples was determined by portable X-ray fluorescence. Micromycetes were recovered from soil samples by a serial dilution method on Czapek-Dox agar medium. The metal resistance spectrum of fungal isolates was investigated for 56.2 mg L^{-1} Cd, 63.5 mg L^{-1} Cu, 10 mg L^{-1} Hg, 518 mg L^{-1} Pb, and 490 mg L^{-1} Zn, individually added to Czapek-Dox agar medium. Molecular identification of the metal resistant isolates (Tolerance Index – TI $\geq$ 0.5) was performed using the ITS region. Hierarchical Clustering Analysis was used to compare metals resistance patterns with fungi phylogeny. A set of 7 micromycetes was selected for minimum inhibitory concentration (MIC) assay, based on their superior resistance for Hg and/or multiple metals. The efficacy of Hg^{2+} removal and the biosorption capacity by five distinct fungal isolates exhibiting superior Hg resistance, were established in aqueous solution containing 100 mg L^{-1} Hg^{2+}. The concentration of Hg^{2+} in the supernatant was measured by a cold vapor atomic absorption spectrometry method, at 0.5 h, 2 h, 6 h, 12 h, 24 h, and 48 h intervals.

3. Mercury resistance strategies in a *Fusarium oxysporum* resistant isolate

The objectives of Hg-resistant *F. oxysporum* P2.7 isolate (GenBank ID: MT913528) study included: (1) establish the minimum inhibitory concentration of Hg in liquid culture medium, (2) establish the primary resistance strategies (extracellular, intracellular, or biovolatilization) to Cu, Hg, and Zn, and (3) bioinformatic study of the putative fungal mercuric reductase.

Mercury resistance limits of the *Fusarium oxysporum* P2.7 isolate were evaluated using a gradient of Hg concentrations (0, 60, 80 and 100 mg L^{-1} Hg) in the culture medium.

The primary metal resistance strategies in the *F. oxysporum* P2.7 isolate were studied in Luria Bertani (LB) culture medium with 250 mg L^{-1} Cu, 10 and 100 mg L^{-1} Hg, and 150 mg L^{-1} Zn. The culture filtrates and the biomasses, collected at the end of the 48-h exposure to metals, were processed and analysed for the metal content by spectrometric or spectrophotometric methods. An active aerated culture system was designed to capture the volatilized Hg, using Anasorb C300 material in traps attached to this system. To distinguish between the extracellular and intracellular metal fractions, the biomass was washed with a 0.1 M HCl solution, which desorbs the extracellular fraction, and used for metal determination for the intracellular fraction. Possible cellular depositions of Hg were investigated in detail by TEM.

The bioinformatic study of the putative fungal mercuric reductase included generation of a phylogenetic tree for the enzyme protein sequences across the life Domains, inspection of key characteristics for enzyme activity across distinct classes of microorganisms, and protein modelling for the putative enzyme in *Fusarium oxysporum*.

CHAPTER III

Results and discussions

1. Biodeteriorative fungal community of canvas paintings

Twenty-one fungal colonies, belonging to 11 distinct species, 8 genera and two phyla, *i.e.*, Ascomycota (86%) and Basidiomycota (14%), were recovered by a non-invasive sampling technique. Most fungal isolates associated with oil or gouache paintings were represented by *Penicillium*, followed by *Aspergillus*, and *Alternaria* genera. The isolated fungal community mostly reflected diversity and abundance described in previous studies concerning fungi associated with canvas paintings. Additional genera, including *Aureobasidium*, *Bjerkandera*, *Cladosporium*, *Filobasidium*, *Porostereum*, and *Trichoderma*, were also identified. The presence of the identified

species raised concerns regarding indoor air quality, potential health implications, and preservation of artworks.

Based on the frequency and intensity of activity for the analyzed enzymes, caseinases, amylases, and gelatinases were detected as the main biodeteriorative enzymes, facilitating the colonization of canvas paintings by fungi. Furthermore, the activities and intensities of acid phosphatase, N-acetyl-β-glucosaminidase, naphthol-AS-BI-phosphohydrolase, and β-glucosidase were associated with a significant potential in promoting fungal colonization and deterioration of canvas paintings, while esterases and leucine arylamidase were identified as enzymes that may contribute to the biodeterioration process. The enzymatic profile detected for the isolated fungi was similar between the two investigated painting techniques.

The species *Aspergillus clavatus*, *Aspergillus luchuensis*, *Aureobasidium pullulans*, *Bjerkandera adusta*, *Penicillium chrysogenum*, and *Trichoderma citrinoviride* were found to induce discolouration of the blue pigment. By incorporating the bromothymol blue pH indicator in the medium containing blue pigment, it was validated that all tested colonies secreted organic acids in this type of medium. Under these conditions, yellow halos developed around the colonized area the medium, indicating a pH decrease below 6, while in the uncolonized area of the medium, the pH was between 6 and 7.6 (Figure 1). This is the first study to report the blue pigment degradation capacity of fungi associated with canvas paintings, likely due to organic acids secretion. The mechanism can be attributed to the complexation of secreted organic acids with the Al atoms from the outer framework structure of the blue pigment, leading to the release of the inner chromophore, and thus, the loss of the specific color. A distinct alteration was noted for the *T. citrinoviride* MD91F4 isolate in the presence of blue and white pigments, where a discernible yellowish hue change occurred in the medium's coloration. This alteration might have been due to secretion of sorbicillinoids, cyclic polyketides restricted to few distantly related ascomycetes, known for their distinct yellow-orange colour and antioxidant properties, and it represents an additional mechanism responsible for biodeterioration.

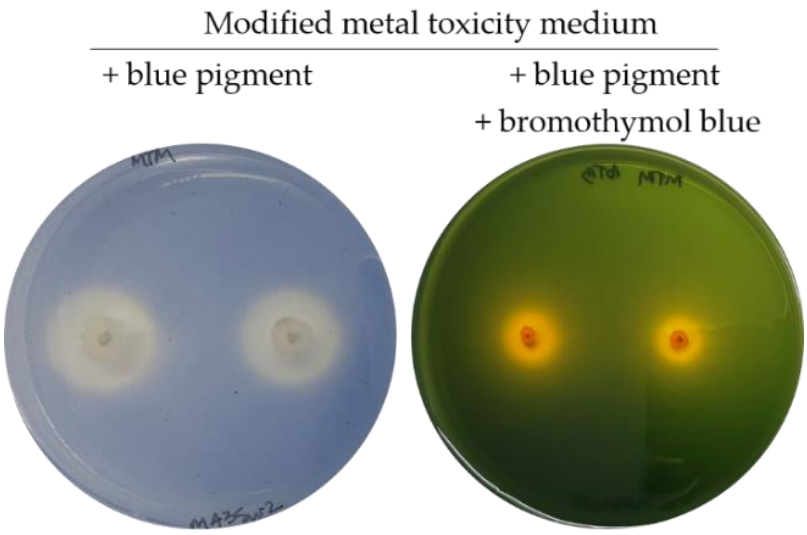

Figure 1. Fungi ability to solubilize the blue pigment, on a modified metal toxicity medium, was the result of organic acid secretion, as highlighted by the bromothymol blue addition to the blue pigment-containing medium (Văcar *et al.*, 2022).

2. Metal resistant fungal community from a Hg-contaminated site

The severe Hg contamination at the study site was confirmed, with values exceeding the industrial soil threshold intervention value by 3.5 to 200 times. Results indicated an exceedingly high ecological risk for Hg, moderate risk for Pb, and minimal risk for Zn, Cu, and Cd, in the rhizosphere soil samples.

The diversity of 32 culturable fungal isolates with moderate or higher resistance (Tolerance Index – TI ≥ 0.5) to at least one metal was depicted in Figure 2. Hierarchical clustering analysis of individual TI for Hg, Pb, Cu, Zn, and Cd underscored the dominance of Ascomycota phylum in heavily Hg-contaminated soil and suggested a general overlap between metal resistance patterns and fungal phylogeny.

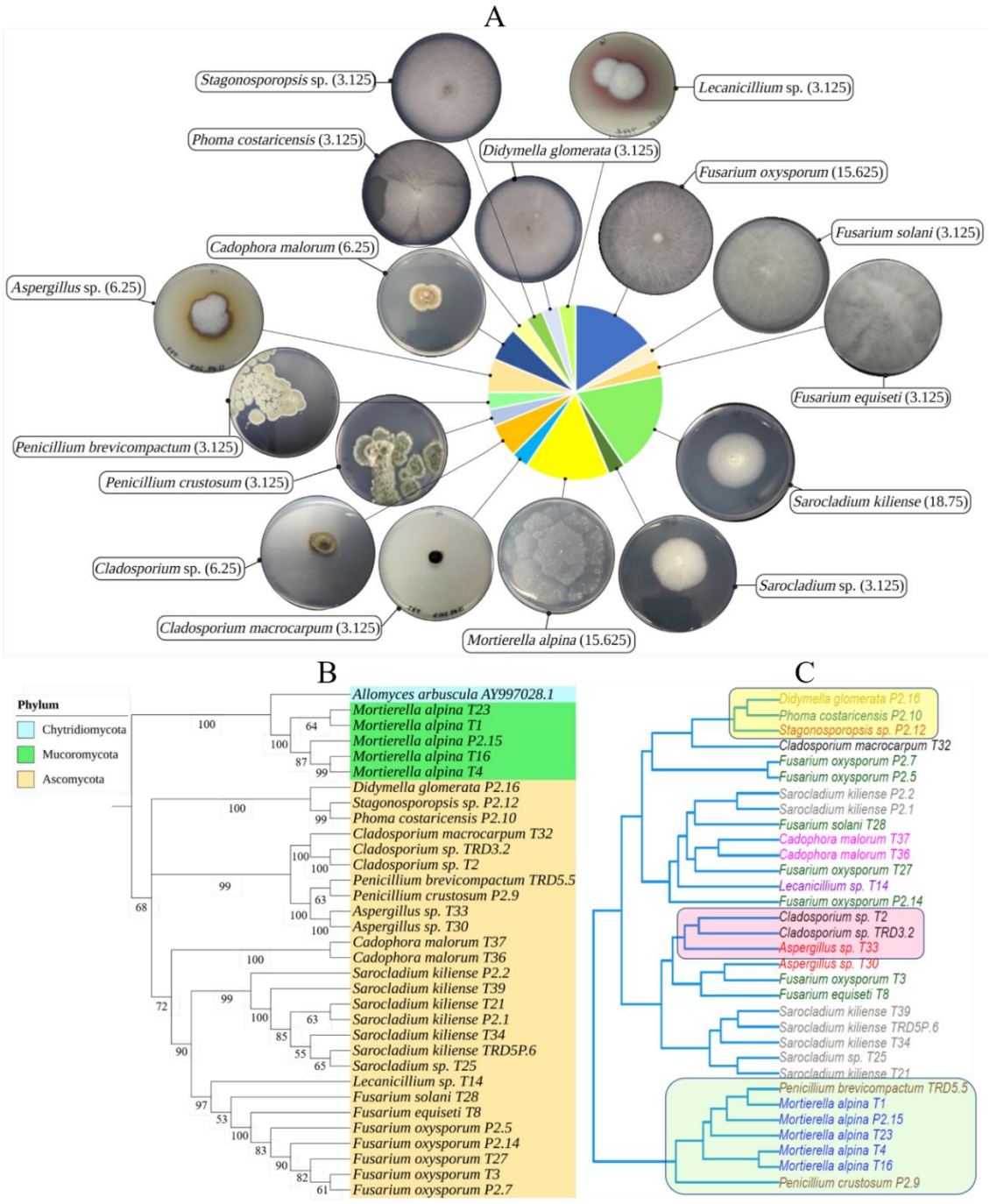

Figure 2. (A) Composition of the isolated fungal community and the phenotypes of 7-day-old cultures on Czapek-Dox agar, with percentages of species given between brackets (created using BioRender software); (B) species phylogeny (neighbor-joining tree) based on internal transcribed spacer sequences (*Allomyces arbuscula* AY997028.1 was used as an outgroup); and (C) dendrogram of hierarchical clustering analysis using the individual tolerance indices (Văcar *et al.*, 2021).

The high frequency of very high and high Hg-resistant phenotypes among the investigated micromycetes demonstrated the selective pressure exerted by Hg in an extremely contaminated background. Isolates with superior metal resistance likely play a crucial ecological role as *in situ* ecological engineers, reducing the bioavailability of these elements and creating habitable microenvironments for the growth of other sensitive microorganisms. *Mortierella alpina* isolates, belonging to the Mucoromycota phylum and occasional symbionts of plants, were rarely recovered from the rhizosphere soil samples, and demonstrated sensitivity to the main contaminants, Hg, Pb, and Cu. It is possible that these isolates might have been engaged by indigenous plant species in symbiotic relationships owing to their responsiveness to root exudates' chemotaxis, regardless of their inferior metal resistance profile. The prevalence of *Fusarium* and other identified genera such as *Penicillium*, *Lecanicillium*, and *Phoma* in current study aligns with previous findings in environments contaminated with Cu, Pb, or Zn. This study reported new fungal species or genera previously unrelated with Hg-contaminated environments, including *Didymella glomerata*, *Lecanicillium* sp., *Fusarium solani*, *F. equiseti*, *Sarocladium* sp., *Penicillium crustosum*, *P. brevicompactum*, *Cadophora malorum*, *Phoma costaricensis*, and *Stagonosporopsis* sp., many of which exhibited very high and high Hg-resistance.

Fusarium oxysporum isolates P2.5 and P2.7 displayed MIC values in potato dextrose agar (mg L^{-1}) of 140 and 200 for Hg, 2353 and 2092 for Zn, and 1568 and 1568 for Pb, respectively. *Phoma costaricensis* isolate P2.10 and *Cladosporium* sp. isolate TRD3.2 exhibited Hg MIC values of 160, while *Didymella glomerata* isolate P2.16 had a MIC of 200 (mg L^{-1}). *Sarocladium kiliense* isolate P2.2 demonstrated MIC values of 200 for Hg, 1036 for Pb, and 381 for Cu, whereas *S. kiliense* isolate TRD5P.6 showed values of 337 and 160 for Cd and Hg, respectively (mg L^{-1}).

The removal and biosorption potential of fresh biomasses developed by five distinct fungal isolates were evaluated in 100 mg L^{-1} Hg^{2+} aqueous solution under shaking conditions (120 rpm), over a 48-h contact period (Figure 3). Within 30 minutes, the fungal biomasses removed between 28% and 52% of the Hg^{2+}. *Didymella glomerata* P2.16 biomass exhibited the highest removal efficiency, 93%, after 2 hours of incubation. The absorption equilibrium was almost attained within 12 hours by all isolates' biomasses. By the end of the incubation period, the removal capacities of fresh fungal biomasses were: 97 ± 0.4% (*D. glomerata*) > 62 ± 5.1% (*F. oxysporum*) ≈ 61 ± 3.9% (*Cladosporium* sp.) > 56 ± 5.0% (*Phoma costaricensis*) > 47 ± 8.0% (*S. kiliense*)

(mean ± 95% confidence level, n = 3). The biosorption capacities for Hg^{2+} ranged from 33.8 ± 5.8, for *P. costaricensis*, to 54.9 ± 11 mg g^{-1} d.w., for *S. kiliense* (mean ± 95% confidence level, n=3).

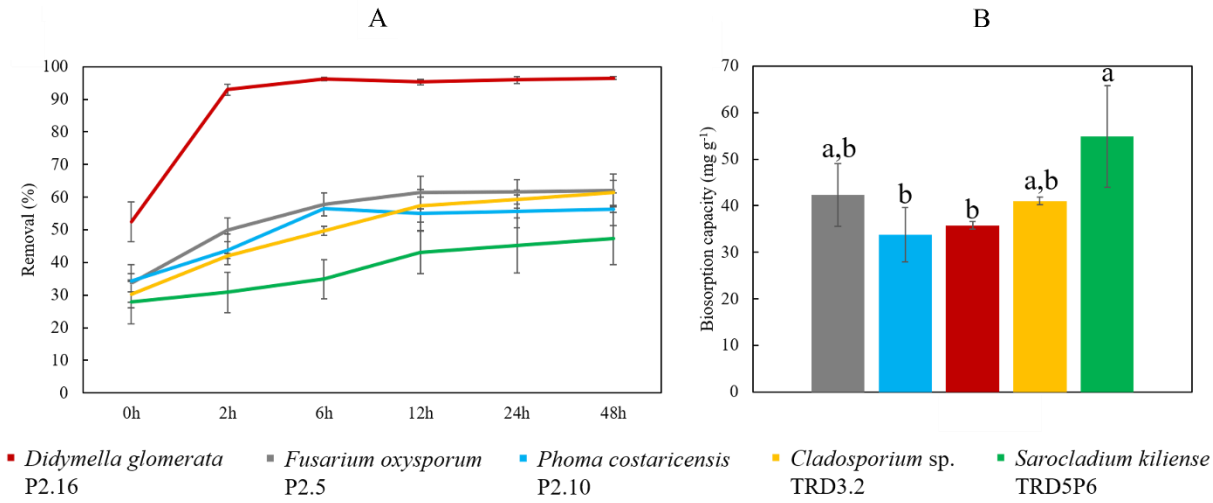

Figure 3. Mercury biosorption potential of five fungal isolates' live biomasses from 100 mg L^{-1} Hg^{2+} aqueous solution over 48 h, 120 rpm agitation: (**A**) removal and (**B**) biosorption capacity; the values represent means, the error bars represent confidence intervals (n = 3, 95% confidence level) and bars with different letters are significantly different (confirmed by Tukey test, $p < 0.017$) (Văcar *et al.*, 2021).

3. Mercury resistance strategies in a *Fusarium oxysporum* resistant isolate

The Hg MIC, representing the concentration of Hg in the medium at which the fungal growth is arrested, was 100 mg L^{-1} Hg in PDB medium for the *Fusarium oxysporum* P2.7 isolate.

The Hg^{2+} removal efficacy and biosorption capacity (Q) of the *Fusarium oxysporum* P2.7 isolate biomass were 81.53% and 9.66 mg Hg g^{-1} d.w, respectively, when cultivated in 200 mL LB medium spiked with 100 mg L^{-1} Hg^{2+}, for 48 h, at 28°C, 120 rpm agitation. Of the total Hg fraction interacting with the biomass 47.57% was removed by extracellular immobilization, 30.4% by intracellular accumulation, and possibly 22.03% by biovolatilization.

The TEM micrographs highlighted the typical structure of the cell wall in control hyphae (Figure 4A). The cell walls of the Hg^{2+}-treated hyphae (Figure 4B, C) appear to lose integrity, as the mannoprotein layer was less electron-dense than in control cells, indicating partial disintegration of this layer. Other signs of Hg toxicity observed were complete detachment of the plasma membrane from the cell wall, or disintegration of the membranous organelles. Remarkably, electron-dense granules, ranging between 11 and 60 nm, were observed at the external

mannoprotein layer of the cell wall, at the exterior of the plasma membrane, and intracellularly in the region of the disintegrated organelles, only in the Hg^{2+}-treated cells. It is likely that the electron-dense granules represent aggregates of Hg^0, due to their circular shape, or other Hg-compounds, as these were observed only in the Hg-treated cells and seem to be associated with signs of cellular toxicity across the main cellular components.

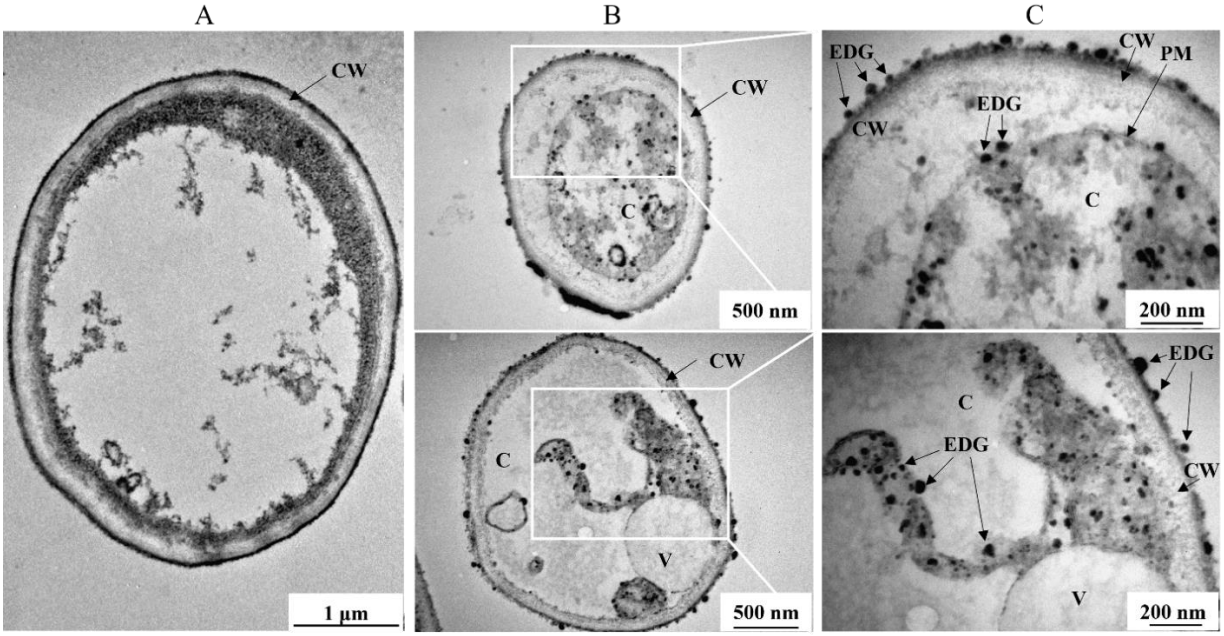

Figure 4. Transmission electron micrographs of cross sections of *Fusarium oxysporum* P2.7 isolate (A) control cell, and (B) cells treated with 100 mg L^{-1} Hg^{2+} for 48 h in LB culture medium, detailed in (C) insets; CW - cell wall, V - vacuole, C - cytoplasm, PM - plasma membrane, EDG - electron-dense granules.

The Hg concentrations in the culture media at the end of experiment (48 h) with *Fusarium oxysporum* P2.7 isolate in 50 mL culture volume with 10 and 100 mg L^{-1} Hg^{2+}, and 120 rpm, were statistically significant lower ($p<0.001$) in the inoculated than in uninoculated treatment, at both initial Hg concentrations. The inoculated variants showed a removal efficacy of the micromycete's biomass of 93.73 ± 0.88% and 83.09 ± 0.62% at 10 and 100 mg L^{-1} Hg, respectively (mean ± SD, n=3). The Hg^{2+} biosorption capacities (mg g^{-1} d.w) of the micromycete's biomass were 0.288 ± 0.015 and 4.75 ± 0.793, at 10 and 100 mg L^{-1} Hg, respectively. The biomass retained 9.38 ± 0.72% and 12.77 ± 3.29%, while 5.18 ± 0.92% and 14.68 ± 0.69% remained residual in the culture medium, at 10 and 100 mg L^{-1} Hg^{2+}, respectively (mean ± SD, n=3). Biovolatilization was

calculated to be responsible for removal of 26.45 ± 0.42% and 5.29 ± 4.2%, at 10 and 100 mg L^{-1} Hg, respectively (mean ± SD, n=3).

At the non-inhibitory 10 mg L^{-1} Hg^{2+}, the response was likely targeted towards a mechanism promoting Hg^{2+} reduction and volatilization as Hg^{0}, since volatilization (26.45%) accounted for the resistance strategies more than biomass retention (9.38%). Alternatively, the cells exposed to the inhibitory 100 mg L^{-1} Hg^{2+}, might have initially directed their response towards Hg^{2+} reduction, rendering 5.29% biovolatilization, until the population of cells was progressively inactivated due to the toxic effects of Hg. Subsequently, the inactivated biomass might have acted as a passive adsorbent until complete saturation, in line with the higher biosorption capacity of the biomass at this concentration.

The change in metals concentration (250 mg L^{-1} Cu, 10 mg L^{-1} Hg, and 150 mg L^{-1} Zn initial) in the 50 mL LB actively aerated cultures was monitored at the time of metal addition (0 h), and at the end of the incubation period (48 h) (Figure 5A-C). The removal efficacies were 6.84 ± 0.99% for Cu, 90.67 ± 3.88% for Hg, and 4.67 ± 2.21% for Zn (mean ± SD, n=6) (Figure 5D). However, the removal efficacy of *F. oxysporum* P2.7 isolate was statistically significant different only for Hg, between the uninoculated and inoculated treatments ($p<0.05$), under actively aerated conditions. The biosorption capacities of *F. oxysporum* P2.7 isolate in LB medium contaminated with 250 mg L^{-1} Cu, 10 mg L^{-1} Hg, and 150 mg L^{-1} Zn, were 13.2 ± 1.19 mg Cu g^{-1} d.w., 2.51 ± 0.09 mg Hg g^{-1} d.w., and 2.87 ± 0.65 mg Zn g^{-1} d.w., respectively (mean ± SD, n=3).

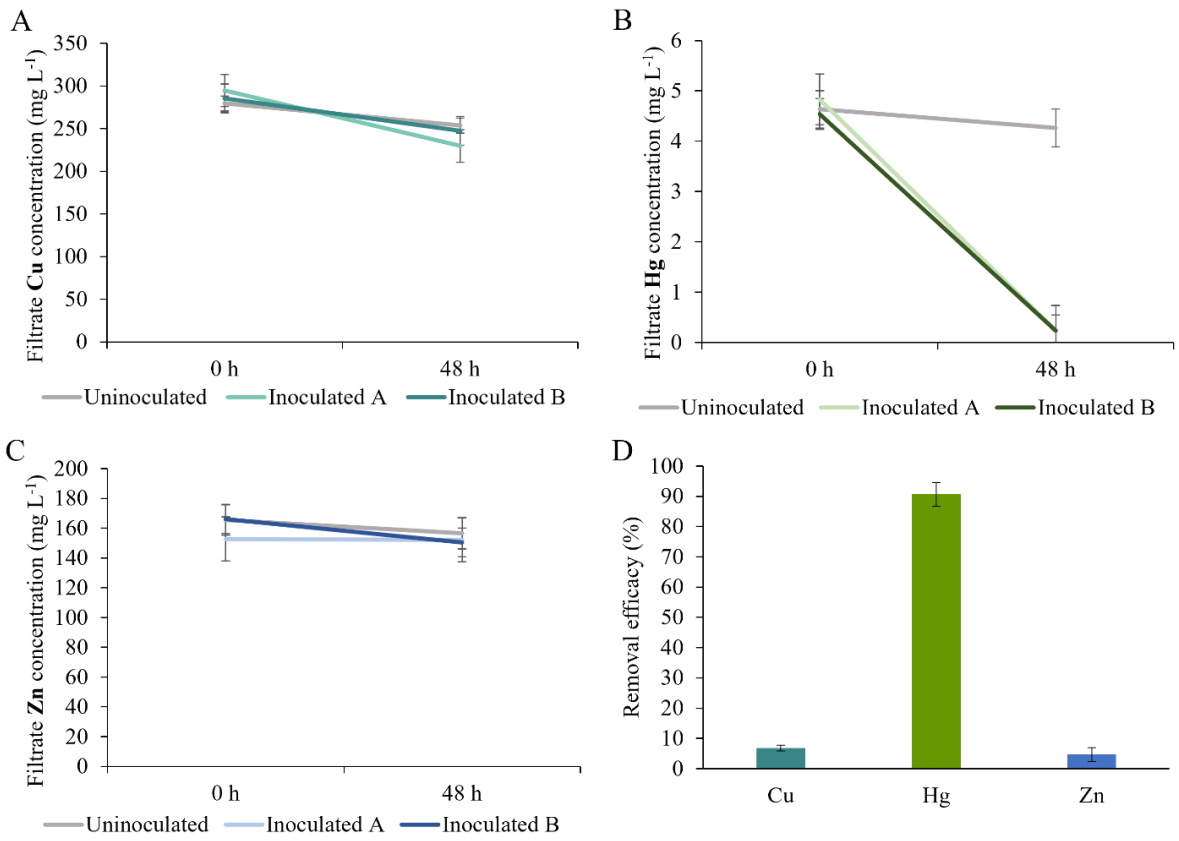

Figure 5. Concentrations of Cu (A), Hg (B), and Zn (C) in the *Fusarium oxysporum* P2.7 isolate culture filtrates measured at the start (0 h) and at the end (48 h) of the experiment, in uninoculated and inoculated A and B variants. (D) Removal efficacy (%) of the *Fusarium oxysporum* isolate P2.7 for Cu, Hg, and Zn at the end of the 48 h of incubation period; the values were expressed as mean ± SD (n=6). The cultures were obtained in LB medium, at 28°C, actively aerated for 5 days, when 250 mg L^{-1} Cu, 10 mg L^{-1} Hg, or 150 mg L^{-1} Zn were spiked and further incubated for 48 h. The error bars represent SD (mean ± SD, n=3).

The main resistance strategies to Cu, Hg, and Zn, of the *F. oxysporum* P2.7 isolate were evaluated based on the elements' concentrations detected in the type A (the total biosorption) and type B (intracellular metal fraction) biomasses (Figure 6). The Cu was completely found immobilized onto the cell walls of the micromycete's biomass, in proportion of 99.99 ± 0.01% (mean ± SD, n=3). Only 14.55 ± 8.88% of the detected Hg was associated with the extracellular fraction, while 48.93 ± 7.07% was associated with the intracellular fraction, rendering a total immobilization to the biomass of 63.48% (mean ± SD, n=3). An important Hg fraction, 36.51 ± 3.11%, was associated with the process of volatilization, captured by the Hg-traps (mean ± SD,

n=3). Similar to Cu, Zn was mostly detected in the extracellular fraction, 93.03 ± 3.02%, while only 6.97 ± 3.02% was detected inside the cells (mean ± SD, n=3).

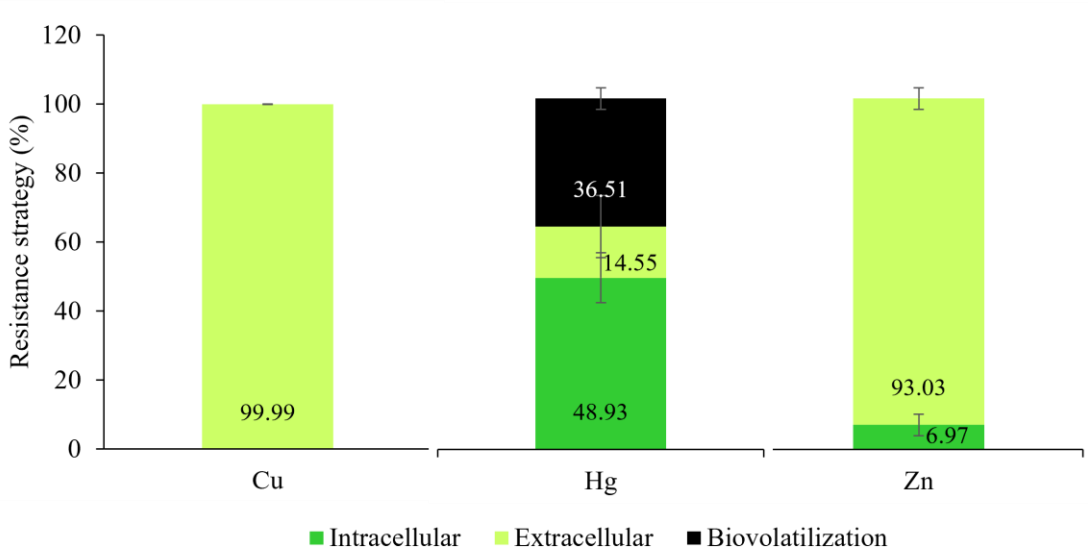

Figure 6. The main resistance strategies of *Fusarium oxysporum* P2.7 isolate after 48 h exposure to 250 mg L^{-1} Cu, 10 mg L^{-1} Hg, and 150 mg L^{-1} Zn, respectively, in LB medium actively aerated cultures. The error bars represent SD (mean ± SD, n=3).

Overall, the results obtained in liquid cultures with metals indicated that *F. oxysporum* P2.7 isolate adapted the main Hg resistance strategies depending on the culture conditions and initial Hg concentration. Extracellular immobilization was employed as a first defense strategy, sequestering Hg^{2+} in the cell wall, followed by permeation into the cytosol, where reduction to Hg^0 followed by volatilization might have occurred. The micromycete's resistance against Cu and Zn stress was attributed to avoidance strategies, with limited to no intracellular uptake, since most quantity of these elements' interacting with the biomass was associated with the extracellular fraction.

The Hg^{2+} biovolatilization in the *F. oxysporum* P2.7 isolate was an inferred process contributing to its highly Hg resistant phenotype. Resistance to Hg acquired through biovolatilization was previously reported in micromycete species. However, thorough characterization of the fungal mechanisms responsible for Hg^{2+} reduction was not reported. The ENH73124.1 NCBI entry (amino acid sequence) was found annotated as mercuric reductase (MerA) in the genome of *F. oxysporum*, without biochemical and genetic characterization, and it

was further used to perform a bioinformatic comparative study with the well-characterized bacterial enzyme.

A phylogenetic analysis of MerA across the three life Domains was employed to disclose the evolutionary pathway of the putative enzyme in Fungi, relative to Bacteria and Archaea. A possible common ancestor for fungal and cyanobacterial MerA sequences was indicated. The majority of fungal MerA sequences shared the conserved CLNVGC motif of the catalytic site with Cyanobacteria, distinct form the CVNVGC conserved in Bacteria and Archaea, suggesting a common origin of the MerA mechanism for Fungi and Cyanobacteria. The lack of the carboxy-terminal Cys pair, in both fungal and cyanobacterial primary structure of MerA, critical for the bacterial enzyme activity, supported the hypothesis of a distinct mechanism from the canonical one in bacteria. This assumption was consolidated by a study reporting MerA-glutaredoxin interactions as viable alternative for the Hg^{2+}-reduction mechanism, in the *Synechocystis* spp. PCC6803 cyanobacterium (Marteyn *et al.*, 2013). It was hypothesized that MerA might be glutathionylated upon Hg^{2+} reduction, then deglutathionylated by the glutaredoxin enzyme Grx1, as both MerA and Grx1 were crucial for the cell survival in the presence of Hg. Moreover, the glutathionylation/deglutathionylation switch of enzyme activity is a biological process representative for eukaryotes (Marteyn *et al.*, 2013).

Modelling of the putative MerA of *F. oxysporum* sequence predicted an expected homo-dimeric configuration (Figure 7). The quaternary structure of the predicted model of *F. oxysporum* putative MerA appeared to match that of the enzyme with crystalized structure in *Pseudomonas aeruginosa*. Moreover, the inner localization of the two Cys of the catalytic site, within the enzyme, was consistent between these models. The superposition of these two models supported the matching of their configuration, although slight differences could be observed in the tertiary structure, as distinctive angles of the peptide chains folds.

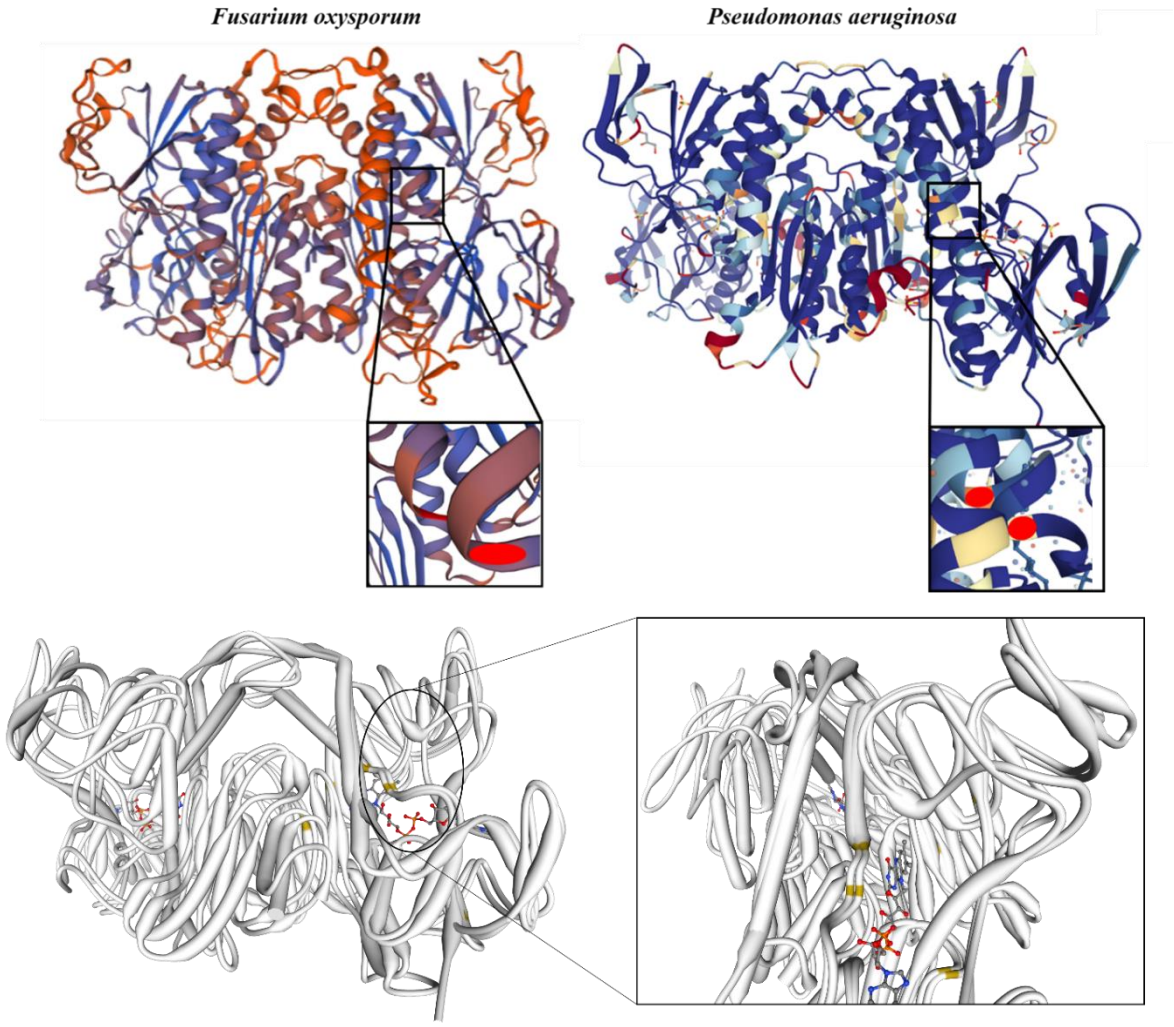

Figure 7. MerA models predicted with SWISS-MODEL for the putative MerA in *Fusarium oxysporum* and canonical MerA of *Pseudomonas aeruginosa* (cartoon style, top); superposed models containing the FAD molecule, with blue and red (rope style, bottom); the insets highlight the positions of the conserved cysteine residues of the catalytic core (red patches top, yellow rings bottom).

CHAPTER IV

Conclusions

The study of fungi associated with canvas paintings, dating from the 18th-20th centuries, brought important contributions to understanding the role of micromycetes in biodeterioration processes. The originality of this study consists in the comprehensive description of fungal metabolic processes involved in biodeterioration, based on a broad enzymatic and pigment

solubilisation screening. Ascomycota representatives, mostly *Penicillium* followed by *Aspergillus* and *Alternaria* genera, were found to dominate the abundance of fungi isolated, while the overall diversity was common for the indoor museal environment. Multiple key enzymes, associated with the process of biodeterioration, were detected with strong activities, indicating that the studied artworks were at considerable risk: caseinases, amylases, gelatinases, acid phosphatases, N-acetyl-glucosaminidases, naphthol-AS-BI-phosphohydrolases, and β-glucosidases. Moreover, blue pigment discoloration capacity was common among the fungal isolates. The phenomenon was likely due to metal complexation, from pigment composition, by the secreted organic acids. Another mechanism that may be responsible for irreversible aesthetic alteration of canvas paintings was pigment secretion. In perspective, the collection of fungal isolates could serve for in depth characterization of biochemical mechanisms and their resulting effects in individual constituents of paintings composition. Additionally, it could aid the study of inactivation technologies efficacy to promote conservation practices.

The study of metal-resistant micromycetes, native to a historically Hg and metal contaminated site, advanced their significant potential for bioremediation purposes, particularly in addressing substrates highly contaminated with Hg. Thirty-two metal-resistant micromycetes isolates were recovered from contaminated soil samples, by classical cultivation techniques, and molecularly identified. The fungal isolates' resistance spectrum and degree to Cd, Cu, Hg, Pb, and Zn, reflected the soil ecological risk indices of these elements at the study site, indicating that the fungal population was well adapted to the toxic conditions. Representatives of Ascomycota were dominant in the analysed population and the metal-resistance patterns overlapped phylogenetically in general. Removal of Hg^{2+} from aqueous substrate at the end of a 48 h treatment was demonstrated with 47-97% efficacy rates and 33.8-54.9 mg Hg g^{-1} d.w. biosorption capacities for a set of five selected micromycetes. These findings underscore the promising role of identified fungal species as effective mycoremediators for highly Hg-contaminated aqueous substrates, suggesting their potential application in environmental restoration efforts. Further research should focus on detailed investigations of molecular and biochemical mechanisms involved in single- or multi-metal resistance in these isolates. The understanding of specific determinants of metal resistance is essential prior controlled up-scale of mycoremediation technologies.

The study of highly metal-resistant *Fusarium oxysporum* P2.7 isolate for its resistance limits and strategies, removal efficiency and biosorption capacity for Hg, combined with the

bioinformatic examination of the putative fungal mercuric reductase, represents a valuable contribution in understanding micromycetes' interaction with Hg and in novel adsorbent materials field. The use of active aerated liquid cultures coupled with Hg-traps is an innovative approach in the study of Hg biovolatilization process. The isolate exhibited high resistance to Hg, as its growth was arrested at 100 mg L^{-1} Hg in liquid medium. Moreover, the micromycete's biomass proved highly effective for the removal of Hg (81.53-93.73%), in the presence of nutrients in the liquid substrate, irrespective of the initial Hg concentration. The primary resistance strategies in the *F. oxysporum* P2.7 isolate against Hg were cellular immobilization (extracellular sequestration and intracellular uptake) and probably biovolatilization. However, the degree of contribution of these resistance strategies varied with initial Hg^{2+} concentration and culture volume and aeration conditions. Avoidance strategies and/or extracellular immobilization were employed by the micromycete against Cu and Zn stress. Nevertheless, Cu biosorption capacities, relevant for development of remediation applications, were established for the *F. oxysporum* P2.7 isolate's biomass. A putative mercuric reductase protein sequence, retrieved from the genome *of F. oxysporum*, is likely the homologue for the well-described bacterial Hg^{2+}-reducing enzyme, based on the presence of the conserved catalytic motif, the predicted cytosolic localization, and the conformation of the modelled protein. Phylogenetic and structural analyses indicated a possible early common origin of this enzyme for Cyanobacteria and Fungi clades, implying a distinct mechanism of Hg^{2+} reduction compared to that of bacteria. The study of fungal Hg reduction and volatilisation is fundamental for understanding this less-explored mechanism in fungi. A thorough characterization of Hg reduction mechanism in fungi would further unlock the progress of mycoremediation techniques and would help to understand the role of microorganisms in the global cycle of Hg speciation.

Dissemination

Articles published in ISI indexed journals (included in the PhD thesis)

as first author

[*]**Văcar, C.L.**, Covaci, E., Chakraborty, S., Li, B., Weindorf, D.C., Frențiu, T., Pârvu, M., Podar, D. Heavy Metal-Resistant Filamentous Fungi as Potential Mercury Bioremediators. *Journal of Fungi* 2021, *7*, 386. https://doi.org/10.3390/jof7050386, **IF** 5.816 (2020).

[*]**Văcar, C.L.**, Mircea, C., Pârvu, M., Podar, D. Diversity and Metabolic Activity of Fungi Causing Biodeterioration of Canvas Paintings. *Journal of Fungi* 2022, *8*, 589. https://doi.org/10.3390/jof8060589, **IF** 5.724 (2021).

as first author with equal contribution ([†])

[*]Tiodar, E.D.[†], **Văcar, C.L.**[†], Podar, D**.** Phytoremediation and Microorganisms-Assisted Phytoremediation of Mercury-Contaminated Soils: Challenges and Perspectives. *International Journal of Environmental Research and Public Health* 2021, *18*, 2435. https://doi.org/10.3390/ijerph18052435, **IF** 4.614 (2021).

Articles published in ISI indexed journals (not included in the PhD thesis)

Văcar, C.L.[†], Ciorîță, A.[†], Tudoran, C., Podar, D., Carpa, R., Leoștean, C., Kacso, I., Mircea, C. Compact cold atmospheric pressure plasma cleaner suited for inhibiting bacterial biodeteriogens from paper archives. *Journal of Cultural Heritage* 2023, *62*, 198-205. https://doi.org/10.1016/j.culher.2023.05.027, **IF** 3.1 (2022).

Article published in ISI indexed journals, as contributor author

Tiodar, E.D., Chiriac, C.M., Pošćić, F., **Văcar, C.L.**, Balázs, Z.R., Coman, C., Weindorf, D.C., Banciu, M., Krämer, U., Podar, D. Plant colonizers of a mercury contaminated site: trace metals and associated rhizosphere bacteria. *Plant and Soil* 2024, https://doi.org/10.1007/s11104-024-06552-7, **IF** 4.9 (2022).

Selective bibliography

Barkay, T., Miller, S. M., Summers, A. O., 2003. Bacterial mercury resistance from atoms to ecosystems. FEMS Microbiology Reviews 27, 355-384, doi:10.1016/s0168-6445(03)00046-9.

Chang, J., Duan, Y., Dong, J., Shen, S., Si, G., He, F., Yang, Q., Chen, J., 2019. Bioremediation of Hg-contaminated soil by combining a novel Hg-volatilizing *Lecythophora* sp. fungus, DC-F1, with biochar: Performance and the response of soil fungal community. Science of The Total Environment 671, 676-684, doi:10.1016/j.scitotenv.2019.03.409.

Chang, J., Shi, Y., Si, G., Yang, Q., Dong, J., Chen, J., 2020. The bioremediation potentials and mercury(II)-resistant mechanisms of a novel fungus *Penicillium* spp. DC-F11 isolated from contaminated soil. Journal of Hazardous Materials 396, 122638, doi:10.1016/j.jhazmat.2020.122638.

Fermo, P., Comite, V., 2022. Indoor air quality in heritage and museum buildings. Handbook of Cultural Heritage Analysis. Springer, pp. 1003-1031.

Fomina, M., Gadd, G. M., 2014. Biosorption: current perspectives on concept, definition and application. Bioresource Technology 160, 3-14, doi:10.1016/j.biortech.2013.12.102.

Gadd, G. M., 2009. Biosorption: critical review of scientific rationale, environmental importance and significance for pollution treatment. Journal of Chemical Technology and Biotechnology 84, 13-28, doi:10.1002/jctb.1999.

Kavkler, K., Humar, M., Kržišnik, D., Turk, M., Tavzes, Č., Gostinčar, C., Džeroski, S., Popov, S., Penko, A., Gunde - Cimerman, N., Zalar, P., 2022. A multidisciplinary study of biodeteriorated Celje Ceiling, a tempera painting on canvas. International Biodeterioration and Biodegradation 170, 105389, doi:10.1016/j.ibiod.2022.105389.

Kumar, V., Dwivedi, S. K., 2021. Mycoremediation of heavy metals: processes, mechanisms, and affecting factors. Environmental Science and Pollution Research 28, 10375-10412, doi:10.1007/s11356-020-11491-8.

Lian, P., Guo, H.-B., Riccardi, D., Dong, A., Parks, J. M., Xu, Q., Pai, E. F., Miller, S. M., Wei, D.-Q., Smith, J. C., 2014. X-ray structure of a Hg^{2+} complex of mercuric reductase (MerA) and quantum mechanical/molecular mechanical study of Hg^{2+} transfer between the C-terminal and buried catalytic site cysteine pairs. Biochemistry 53, 7211-7222, doi:10.1021/bi500608u.

Marteyn, B., Sakr, S., Farci, S., Bedhomme, M., Chardonnet, S., Decottignies, P., Lemaire, S. D., Cassier-Chauvat, C., Chauvat, F., 2013. The *Synechocystis* PCC6803 MerA-like enzyme operates in the reduction of both mercury and uranium under the control of the glutaredoxin 1 enzyme. Journal of Bacteriology 195, 4138-4145, doi:10.1128/JB.00272-13.

Panagos, P., Van Liedekerke, M., Yigini, Y., Montanarella, L., 2013. Contaminated Sites in Europe: Review of the Current Situation Based on Data Collected through a European Network. Journal of Environmental and Public Health 2013, 158764, doi:10.1155/2013/158764.

Rajendran, S., Priya, T. A. K., Khoo, K. S., Hoang, T. K. A., Ng, H.-S., Munawaroh, H. S. H., Karaman, C., Orooji, Y., Show, P. L., 2022. A critical review on various remediation approaches for heavy metal contaminants removal from contaminated soils. Chemosphere 287, 132369, doi:10.1016/j.chemosphere.2021.132369.

Skóra, J., Gutarowska, B., Pielech-Przybylska, K., Stępień, Ł., Pietrzak, K., Piotrowska, M., Pietrowski, P., 2015. Assessment of microbiological contamination in the work environments of museums, archives and libraries. Aerobiologia 31, 389-401, doi:10.1007/s10453-015-9372-8.

Sterflinger, K., Piñar, G., 2013. Microbial deterioration of cultural heritage and works of art—tilting at windmills? Applied Microbiology and Biotechnology 97, 9637-9646, doi:10.1007/s00253-013-5283-1.

Tiodar, E. D., Văcar, C. L., Podar, D., 2021. Phytoremediation and Microorganisms-Assisted Phytoremediation of Mercury-Contaminated Soils: Challenges and Perspectives. International Journal of Environmental Research and Public Health 18, 2435, doi:10.3390/ijerph18052435.

Văcar, C. L., Covaci, E., Chakraborty, S., Li, B., Weindorf, D. C., Frențiu, T., Pârvu, M., Podar, D., 2021. Heavy Metal-Resistant Filamentous Fungi as Potential Mercury Bioremediators. Journal of Fungi 7, 386, doi:10.3390/jof7050386.

Văcar, C. L., Mircea, C., Pârvu, M., Podar, D., 2022. Diversity and Metabolic Activity of Fungi Causing Biodeterioration of Canvas Paintings. Journal of Fungi 8, 589, doi:10.3390/jof8060589.

Wang, L., Hou, D., Cao, Y., Ok, Y. S., Tack, F. M. G., Rinklebe, J., O'Connor, D., 2020. Remediation of mercury contaminated soil, water, and air: A review of emerging materials and innovative technologies. Environment International 134, 105281, doi:10.1016/j.envint.2019.105281.